AD-A117 837 NAVAL SURFACE WEAPONS CENTER DAHLGREN VA F/G 8/5
EVALUATION OF GEODETIC PRODUCTS PRODUCED BY THE NSWC REDUCTION --ETC(U)
JUN 81 S L SMITH, T I HICKS
UNCLASSIFIED NSWC/TR-81-260 NL

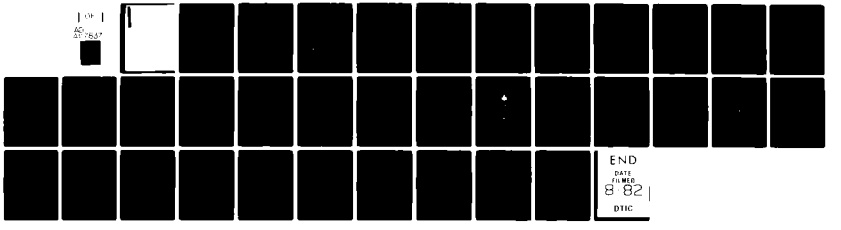

UNCLASSIFIED

SECURITY CLASSIFICATION OF THIS PAGE *(When Data Entered)*

REPORT DOCUMENTATION PAGE		READ INSTRUCTIONS BEFORE COMPLETING FORM
1. REPORT NUMBER NSWC TR 81-260	2. GOVT ACCESSION NO. AD-A117837	3. RECIPIENT'S CATALOG NUMBER
4. TITLE *(and Subtitle)* Evaluation of Geodetic Products Produced by the NSWC Reduction of SEASAT Radar Altimeter Data		5. TYPE OF REPORT & PERIOD COVERED Final 6. PERFORMING ORG. REPORT NUMBER
7. AUTHOR(s) Samuel L. Smith III Thomas I. Hicks		8. CONTRACT OR GRANT NUMBER(s)
9. PERFORMING ORGANIZATION NAME AND ADDRESS Naval Surface Weapons Center (K12) Dahlgren, Virginia 22448		10. PROGRAM ELEMENT, PROJECT, TASK AREA & WORK UNIT NUMBERS 63701B
11. CONTROLLING OFFICE NAME AND ADDRESS Defense Mapping Agency Washington, D.C. 20360		12. REPORT DATE June 1981 13. NUMBER OF PAGES 30
14. MONITORING AGENCY NAME & ADDRESS*(if different from Controlling Office)*		15. SECURITY CLASS. *(of this report)* Unclassified 15a. DECLASSIFICATION/DOWNGRADING SCHEDULE

16. DISTRIBUTION STATEMENT *(of this Report)*

Approved for public release; distribution unlimited.

17. DISTRIBUTION STATEMENT *(of the abstract entered in Block 20, if different from Report)*

18. SUPPLEMENTARY NOTES

19. KEY WORDS *(Continue on reverse side if necessary and identify by block number)*

SEASAT
Satellite Radar Altimeters
Ocean Geodesy
Geoid Height
Vertical Deflection

20. ABSTRACT *(Continue on reverse side if necessary and identify by block number)*

An estimation is made of the possible errors associated with the processing by NSWC of raw SEASAT altimetry data to produce ocean geodetic data, e.g. geoid heights and vertical deflections. Also the noise level of the SEASAT radar altimetry is estimated. Then the SEASAT geodetic data are examined for self-consistency on repeat-track sequences and compared with other independent geodetic data obtained from ocean gravity surveys by ships. Anomalies in the comparisons are examined to determine probable causes.

DD FORM 1 JAN 73 1473 EDITION OF 1 NOV 65 IS OBSOLETE
S/N 0102-LF-014-6601

UNCLASSIFIED

SECURITY CLASSIFICATION OF THIS PAGE *(When Data Entered)*

Finally, the accuracy obtainable from a large, well edited set of SEASAT data (or similar radar altimeter satellite such as GEOSAT without further orbit improvement) is estimated to be the following:

0.5-1.5 m rms in geoid height

0.5-2.0 arc sec rms in vertical deflection

FOREWORD

This work was performed in the Space and Ocean Geodesy Branch, Space and Surface Systems Division, Strategic Systems Department of the Naval Surface Weapons Center (NSWC) under the sponsorship of the Defense Mapping Agency via P.E./Project/Task No. 63701B/3204/240. The authors wish to express appreciation to Richard J. Anderle for guidance and advice in the preparation of this report and to Elodie Colquitt for providing the tracking-data summary in Table 3.

This report was reviewed by R. L. Kulp, Head, Space and Ocean Geodesy Branch, and D. R. Brown, Jr., Head, Space and Surface Systems Division.

Released by:

O. F. BRAXTON, Head
Strategic Systems Department

CONTENTS

INTRODUCTION

The SEASAT oceanographic satellite was launched on 26 June 1978 from Vandenburg Air Force Base, California. SEASAT carried five sensors: a microwave radar altimeter (ALT), synthetic aperture radar (SAR), scanning multifrequency microwave radiometer (SMMR), microwave scatterometer (SCAT), and visual and infrared radiometer (VIR), as well as three separate systems for tracking and orbit determination; a Navy Doppler Beacon, Laser Corner Cube Array, and a NASA Unified S-Band System. A complete description of SEASAT may be found in Reference 1. The principal sensor of interest to the Department of Defense (DOD) geodetic community was the microwave radar altimeter, which was expected under the nominal mission to acquire data to allow DOD to produce an ocean geoid and gridded deflection of vertical values over the world's oceans to at least a 10-nmi spacing. Unfortunately, SEASAT underwent a catastrophic power failure on 10 October 1978, which terminated the mission. Although its lifetime was short, and some data were lost due to other power and attitude problems, SEASAT did produce a sizable ocean data base. The purpose of this report is to give an evaluation of the quality of the geodetic data (along-track geoid height and vertical deflection) produced by the Naval Surface Weapons Center (NSWC) from the SEASAT radar altimeter data base. This analysis should also be valuable in identifying the larger error contributors to the geodetic products and what needs to be done to improve the data processing of proposed future altimeter satellites such as GEOSAT or TOPEX.

PROCESSING

The DOD processing system for SEASAT was originally set up so that the Fleet Numerical Oceanography Center (FNOC), Monterey, California, would initially acquire all the SEASAT data in as near real time as possible for use in its weather/ocean predictions. Furthermore, while processing, they would preprocess the data of geodetic interest using software supplied by the NSWC, Dahlgren, Virginia, and send the output to NSWC. The preprocessing by FNOC reduced the amount of data to be sent across the country and eliminated some redundant processing that otherwise would have been necessary and thus resulted in overall economy for DOD. Start-up problems and the early loss of SEASAT prevented the optimum use of the above-described system, as FNOC obtained most of the data from NASA/GSFC too late for their real-time use, but FNOC still preprocessed the data for geodetic use. The preprocessed SEASAT data were combined by NSWC with precise Doppler orbits and other environmental corrections that had not been applied, such as the tide correction (Reference 2) and along-track sea-surface height, which is an approximation to geoid height, and deflection of the vertical were computed. A description of the preprocessor software is given in Reference 3, and the NSWC processing system is given in Reference 4. Only those parts of the system that resulted in known errors in the final geodetic products or that were evaluated for accuracy will be further mentioned in this report.

ORBITS

The orbits used by NSWC with the SEASAT data were two revolution fits to Doppler tracking data acquired by the DOD TRANET/Geoceiver Tracking Network. Details of the orbit computations are given in Reference 5, as is an estimate of accuracy of 1.5 m rms in the radial component, which is the important component in reduction of SEASAT radar altimeter data to ocean geodetic information.

EDITING AND AGGREGATION OF DATA

A test was implemented in the preprocessor to separate ocean and land data and write them on separate files. The test was based on a predicted orbit and CIA World Map Data Bank I, which does not contain many of the smaller islands and lacks some detail along some coastlines. This resulted in some land contamination being contained in the SEASAT ocean data. Since the radar altimeter was optimized for ocean measurements, it would usually lose lock over land terrain; but before it did, the measurement noise would increase significantly.

The altimeter usually tracked over sea ice, but the measurement noise increased significantly. No test was implemented to eliminate sea-ice data (as could have been done based on the radar automatic gain control (AGC) values) but data taken over land or sea ice should not be used in the final geodetic products.

In an attempt to eliminate data outliers (telemetry (TM) bit errors, noise spikes, etc.) a sliding least-squares linear fit was applied to the raw 10/sec range data with individual data points more than a chosen sigma eliminated from the data set. This test eliminated a number of very bad points, but a number of smaller 1- to 2-m spikes remained in the data base.

The data were then aggregated (by averaging) to two data points per second. Any bad data that remained at this point caused broadened problems after being passed through the Kalman smoother. The effect will be discussed later in the section on the Kalman smoother.

CORRECTIONS

The following sections discuss the corrections selected from those of Reference 4 for special evaluation studies.

Time Bias

A time delay exists between the time a radar return pulse reaches the antenna and the time the pulse is recognized as a legitimate return by the altimeter logic circuits. The value recommended by the SEASAT project engineers based on prelaunch measurements for this time bias was -147.951 msec. (Reference 6). Consistency of intersection analysis is sensitive to this time

bias, and early intersection analysis results at NSWC were not as good as they were expected to be. Also J. G. Marsh (personal communication) at NASA/GSFC found a zero time bias gave better results than the -147.951 msec value. Subsequently, NSWC ran several small samples of SEASAT data with several time biases. Intersection analyses were performed in three oceans (North Pacific, South Pacific, and Indian), and it was found that a time bias of -51 msec gave the most consistent results. An evaluation of various data and techniques by the SEASAT ALT/POD team finally arrived at -79.38 msec as the most probable value (Reference 7). By this time NSWC had already processed much of the SEASAT data with a time bias of -51 msec and did not reprocess it with the -79.38 msec value. This could lead to a maximum error of about 5 cm in the NSWC reduced data but with the average error much smaller.

Ionosphere

The NSWC correction for ionospheric propagation effect on the radar altimeter measurement was made using expressions (in closed form for nadir signals) from Reference 8, where the electron density was scaled by using the predicted sunspot numbers from the Institute of Radio Telecommunications in Boulder, Colorado. The predicted sunspot numbers were used, since the processing system was originally designed for near real-time processing and the real numbers would not yet be available. When SEASAT suffered its premature failure and most data were processed at a later date when the actual numbers were available, the predicted numbers were still used since they were already in the computer file. At the 13.5-GHz frequency of the SEASAT radar altimeter, the maximum correction to be expected is about 20 cm. The data are not available for an exact determination of the errors resulting from the NSWC method; however, the Jet Propulsion Laboratory (JPL), Pasadena, California, computed an ionospheric correction for SEASAT data using an independent method whereby its model was scaled by electron densities inferred from Faraday rotation measurements made in California and Australia each day. Reference 9 gives a discussion of this procedure and compares (in its Figure 1) the JPL and NSWC ionospheric corrections for revolution 1117. The maximum difference is less than 5 cm, and the average difference is much less. Since neither model takes into account possible local nonhomogeneities in the electron content of the ionosphere, it is estimated that their absolute accuracy is of the order of 5 cm rms. This is a pessimistic estimate, and the accuracy is probably much greater.

Troposphere

The range corrections to the radar altimeter measurements due to the neutral atmosphere were made with atmospheric models scaled by surface temperature, pressure, and relative humidity values obtained from worldwide 12-hr gridded fits made by FNOC to all available weather data for the prior 12 hr. The values were interpolated to SEASAT subsatellite points and it is believed that the pressure values, which are the principal contribution to the "dry" part of the troposphere, are well enough behaved to yield errors in the "dry" correction of the order of 2 cm rms.

However, the water vapor content, which causes the "wet" part of the altimeter range correction, is much more variable and more likely to be lost in the broad time and space modeling of the atmosphere by FNOC. Originally it was planned to obtain the "wet" correction from water vapor measurements made by the SEASAT SMMR, but problems with calibration and antenna corrections prevented this measurement from being generally available for altimeter corrections in a timely manner, and the data was processed using FNOC values to make the correction. Subsequent to the NSWC processing of the SEASAT altimeter data, some SMMR data were processed and comparisons of the NSWC corrections using FNOC data, SMMR derived corrections, and isolated radiosone measurements were made in the vicinity of Bermuda and Kwajalein (Reference 10). Wet tropospheric radar altimeter corrections are shown in Table 1. Table 2 gives comparisons at the points of radiosone measurement, where the constant model is an average ocean value, to be used if for any reason the FNOC data is not available.

Table 1. Wet Tropospheric Radar Altimeter Corrections

Rev	Area	Radiosone (cm)	SEASAT SMMR (cm)	Model with FNOC Weather (cm)	Constant Model (cm)
1172	Kwajalein	32.3	34.5	27.9	13.2
1215	"	41.6	38.0	27.8	13.2
1258	"	39.9	37.5	28.4	13.2
1160	Bermuda	19.0	19.2	31.9	13.2
1375	"	33.0	33.0	27.5	13.2

Table 2. Average Differences With Respect to Radiosonde Data

	cm
SMMR	1.7
Model w/FNOC Data	9.6
Constant Model	18.0

On the basis of this limited comparison, it is estimated that using the model with FNOC data yields a correction to the altimeter range measurement of the order of 10 cm rms.

Kalman Smoother

The SEASAT altimeter data at 2/sec averages has a basic noise level (essentially white noise) of 4 to 15 cm, which is a function of sea state, with the higher values associated with higher sea states. More will be said of this altimeter noise later. The Kalman smoother (Reference 11) is used to attempt to eliminate this random noise component from the sea-surface height as well as to provide a method to estimate the along-track deflection of the vertical. If the data are "clean," i.e., do not contain large (~1 m or greater) spikes, as

have been seen in SEASAT data from TM bit errors, land contamination, or other reasons, the Kalman smoother works quite well. However, where these spikes occur, the Kalman smoother tries to even them out and in doing so degrades the final output over a much broader along-track interval. Furthermore, the character of the noise spike loses identity in the smoothed data and might appear to be the effect of a seamount or trench. If in using the final SEASAT output such an effect is suspected due to noncorrelations of the SEASAT data with other data (even other SEASAT data under near repeat conditions), the sigma range word in the Interim Geophysical Data Record (IGDR) file or a plot of the raw geoid height (carried on both the Geophysical Data Record (GDR) and IGDR files) should enable one to determine if noise is the problem. Sea ice in the altimeter field of view usually results in a noise level of 1 m or greater in the raw altimeter data and causes degradation of the final data when it is present. Care should be taken when working with the SEASAT data at those latitudes where ice would be likely.

RESULTS AND EVALUATION

RADAR ALTIMETER NOISE LEVEL

Two methods have been used at NSWC to arrive at an estimate of the basic noise level of the SEASAT radar altimeter. The first involved power spectral density analysis (at NSWC by Peter Ugincius) of the SEASAT geoid height (Reference 12). This analysis over several samples of SEASAT data showed rms noise levels of between 4.3 and 8.4 cm (depending on the sample) being reached at wavelengths of about 30 km. The second method arises from the data editing and aggregating method mentioned earlier. The standard deviation is determined for both the raw altimeter range and significant wave height (SWH) when averaging to obtain the 2/sec data from the 10/sec data. While this variation is not necessarily due only to radar altimeter range noise, due to its short wavelength and time (about 700 m and 1/10 sec) it is thought to be predominantly altimeter range noise. Furthermore, the altimeter range noise is expected to be a function of sea state (Reference 1). Therefore, the raw range standard deviation has been sampled for several passes using the following criteria.

1. All known ice- and land-contaminated data are avoided.
2. The AGC is stable, i.e., no more than ±1 dB variation over the sample.
3. The altimeter SWH value is stable, i.e., not greater than ±1/2 m over the sample.

This resulted in samples usually in the time range of 5 to 20 sec (about 35 to 140 km along track). Also it should be noted that the SWH values used are raw data from the altimeter; that is, they have not yet been corrected for attitude or SWH biases. The resulting data are plotted in Figure 1, and the range over

these samples is from 4 to 14 cm with considerable scatter and an increasing trend with increasing SWH. This result is consistent with the power spectral density analysis and shows that the SEASAT radar altimeter performed considerably better than its design goal of 10 cm range noise.

Ice and land (even partial in the altimeter footprint) for which the altimeter was not designed can increase this range noise up to several meters, and apparently returns through heavy rain can also cause a drastic increase in the range noise, and anomalies in the geodetic products. But by knowing the usual values over open ocean from this study, this is another parameter that can be used to filter the data for precise geodetic determinations.

SEASAT SELF-CONSISTENCY

From revolution 1075 until its failure, SEASAT was in an orbit that provided data from ground tracks that repeated to within the altimeter footprint at about 3-day intervals (43 orbit periods). This provided an excellent opportunity to study the repeatability or self-consistency of the SEASAT geodetic data and a chance to observe the occurrence of unmodeled and uncorrected environmental events. Figures 2, 3, and 4 are around-the-world plots of ge height for the 1st, 3rd, and 8th revolutions of the repeat-track sequence:

Revolution	1198
"	1241
"	1284
"	1327
"	1370
"	1413
"	1456
"	1499

with geographic features marked on the plot for revolution 1198. While the similarity is quite evident and gross features, large land-contamination spikes, and Antarctic ice may be readily seen, the scale of these figures is totally inadequate for detailed quantitative comparison. Note that the data for revolution 1499 ended early when Antarctic ice was encountered. Unexplained loss of data occurred occasionally throughout the mission and is thought to be due to telemetry problems. Figure 5 is a plot of along-track deflection of the vertical for revolution 1198 and the land contamination and ice effects stand out even more clearly. While the Antarctic ice is obvious, it was not definite whether the roughness (noisy data) in the East Siberian and Laptev Seas was due to ice or land contamination, since the data were taken in late summer in the northern hemisphere. An examination of the AGC listings showed that there were significant amounts of ice in these areas as well as some open water. Even in the Antarctic, where ice would be expected, the AGC revealed some small areas of open water. The conclusion that some open water exists in these ice areas is based on knowledge that water leads can and do exist under such conditions, coupled with the return of altimeter AGC and range noise levels to normal ocean values for brief intervals. However, the possibility remains that the altimeter is sensing through storms (rain, snow?) and

the attenuation of the radar signal by the storm causes the drop in AGC and range noise level. Two areas, marked area 1 and area 2 on Figure 2, have been chosen for detailed quantitative comparison. Area 1 is in the Pacific Ocean about 1200 mi off the west coast of the United States and area 2 is off the southeast tip of Africa. The ground track length in each of these areas is between 3500 and 4000 km. Figure 6 is a plot of the geoid heights from each track of the above sequence in area 1 plotted against an arbitrary time scale. It is seen that pass-to-pass shifts occur in the geoid heights, with a total range of slightly over 3 m and a significant tilt is also evident in revolution 1413. These differences were thought to be due to orbit biases, and the mean and standard deviation with respect to revolution 1198 (chosen arbitrarily) was calculated. The mean was 21 cm and standard deviation 1.09 m, which is well within the estimated orbit accuracy quoted earlier (Reference 5). The tilt in revolution 1413 was somewhat disturbing and it was decided to look at the distribution of Doppler tracking for this repeat sequence. Elodie Colquitt (NSWC, personal communication) provided the following table of Doppler tracking:

Table 3. SEASAT Repeat Tracks

Station No.	Station Name	Maximum Elevation (°)	Revolution No. 1198	1241	1284	1327	1370	1413	1456	1499
30939	CHAGOS	63.2		X						X
20	MAHE	20.		X	X	X	X			X
30730	EASTER	88.4	X	X		X	X	X	X	
113	NEW MEXICO	5.0			X	X	X	X	X	
51960	UKIAH	25.		X	X				X	X
30414	CALGARY	9.	X		X	X			X	X
114	ANCHORAGE	53.8	X	X	X	X	X	X	X	X
127	ALEUTIANS	17.2	X	X	X		X	X	X	X
20	MAHE	29.3	X		X	X	X		X	
105	PRETORIA	45.3	X	X	X	X	X		X	X
30730	EASTER	9.7	X	X	X	X	X	X	X	X
30188	HAWAII	65.7		X	X	X	X	X	X	X
127	ALEUTIANS	49.4	X	X	X		X	X	X	X
114	ANCHORAGE	15.2	X	X	X	X	X	X	X	X
TOTAL PASSES			9	11	12	10	11	8	12	11

It is seen that revolution 1413 had the poorest tracking of any pass of the sequence both in quantity and distribution; therefore, the tilt is probably due to lack of good tracking anywhere but in the Alaska area. Figure 7 presents the geoid-height data again for this sequence in area 1, where each revolution and revolution 1198 are compared, with the ordinate scale shifted 8 m. The time scale given is seconds (of day) for revolution 1198 for ease in the comparison of details. The tilt of revolution 1413 is again seen and an extra "bump" occurs on revolution 1284 (arrow) that is not seen on the other revolutions. Figure 8 gives the along-track vertical-deflection plots for revolutions 1413, 1284, and 1241, along with revolution 1198. Differences are seen in revolution 1284 for about 100 sec in the neighborhood of the "bump" in the geoid-height plot. The differences in vertical deflection are plotted in Figure 9 for these three pairs of revolutions (note the change in the ordinate scale). The differences appear random, with a magnitude of about ±1 arc sec, except for the vicinity of the anomaly of revolution 1284. Also note that there is a shift of about 0.25 arc sec due to the tilt of revolution 1413 discussed earlier. In order to seek an explanation for the anomaly of revolution

1284, a listing of all the data and corrections was made. All parameters were stable or smoothly varying throughout this data segment including the altimeter-determined SWH at about 2-3 m, except for the AGC, which rose from 32 to 40 dB in the area of the anomaly and dropped back to 32 dB when the data agreed again. This is possibly a case of a patch of smooth water giving high AGC returns as reported by Townsend (Reference 1), but it is not known why the SWH values did not change.

Figure 10 gives the geoid-height comparison in area 2 for each revolution with revolution 1198 (except revolution 1327, which is missing). The major differences seen here are again the tilt of revolution 1413 and a data anomaly (arrow) on revolution 1499. Figures 11 and 12 compare the vertical deflections and their respective differences, of revolutions 1499, 1370, and 1241 with revolution 1198. First it should be noted that, in general, the differences are somewhat larger than those in area 1 (excluding anomalies). The maximum is almost ±2 arc sec. This is thought to be due to a sea-state effect increasing the altimeter noise level since this area off the coast of Africa had altimeter-measured sea states averaging in the 4- to 5-m SWH range during the time span of this sequence of passes, whereas area I in the Pacific Ocean averaged 2-3 m during the data span. The anomaly of revolution 1499 is quite large and two anomalies show up clearly on Figures 11 and 12 for revolution 1241 that were hardly discernible in Figure 10. Complete data listings were again consulted to seek an explanation for these anomalies. All parameters were nominal except for AGC, SWH, and raw range noise, which exhibited similar characteristics for each anomaly as given in Table 4.

Table 4. Raw Range Noise, AGC, and SWH Parameter Anomalies

Revolution No.	Anomaly Time Span (sec)	Raw Range σ (cm)			AGC (dB)			SWH (m)		
		From	To	Back To	From	To	Back To	From	To	Back To
1499	8	7	164	5	32	27	32	2.2	19.9	3.5
1241 1st	4	5	79	4	32	30	32	3.3	9.0	3.8
1241 2nd	8	7	52	6	32	27	32	3.1	9.4	3.2

This behavior is characteristic of passing over (and sensing through) an intense local rain cell as was determined in the GOASEX experiment (Reference 13) where detailed surface truth and weather data were available for correlation with the SEASAT data. Therefore, it is highly probable that these anomalies are due to local weather conditions. The FNOC wind fields indicated 36-kt winds in the area of the anomaly on revolution 1499. Several other repeat-track sequences have been analyzed as above for the sequence beginning with revolution 1198 with essentially the same results. The overall self-consistency statistics for the repeat-track data just as it comes from NSWC processing is the following:

Geoid height rms 1.9-2.3 m

Vertical deflection rms 1-2 arc sec

If an adjustment to the mean is made to reduce orbit biases (this procedure would reduce any bias, but the orbit has been shown to be the largest contributor), the self-consistency is the following:

Geoid height rms	30-40 cm
Vertical deflection rms	1-2 arc sec

The vertical deflection does not change because a true orbit bias contributes zero vertical deflection and even a relatively large orbit tilt as seen in revolution 1413 contributes only 0.25 arc sec to the vertical deflection.

If the effects on geoid height and vertical deflection discussed for the revolution 1198 sequence due to environmental disturbances were also removed, the above statistics, particularly the vertical deflection, would show some improvement. This was not done because of the amount of labor involved in even a data set as small as the SEASAT repeat-track data. However, the analysis has suggested some refined computer editing that should be done to improve the accuracy of the geodetic products of a future altimetry satellite such as GEOSAT, where the data base is expected to be much too large to attempt human editing of the data.

SEASAT COMPARISONS WITH SHIP DATA

Certain areas of the oceans have been surveyed in detail with shipborne gravimeters, and the gravity data have been reduced to geoid height and vertical deflection (components in the north and east directions) on a closely spaced grid. The data reduction method used requires worldwide data, and the area outside the survey areas is filled in with geodetic models derived from dynamic analysis of satellite orbits. The resulting gridded data has very good accuracy in the shorter wavelengths (up to the survey area dimensions) but may have long wavelength and scale errors due to the models used in the unsurveyed area. For security reasons when using this gridded data base, in the comparisons that follow, all identification has been deleted from the SEASAT data and the plots are made against an arbitrary time scale.

The comparisons are made as follows: the NSWC reduction of SEASAT data produces values of geoid height and along-track components of vertical deflection at about 1/2 sec time (about 3.35 km on the ocean surface) intervals and the position (latitude, longitude) of each point. The gridded geoid-height data base is entered with each point and a bilinear interpolation done to find the corresponding "ship" data to compare with the SEASAT data. The computations for vertical deflection are similarly done with bilinear interpolation in the gridded north and east vertical deflection component tables, but with the added requirement to vectorally combine the two components in the local SEASAT subtrack direction (azimuth) to produce the "ship" along-track vertical deflections.

Figure 13 gives three samples of SEASAT and "ship" geoid-height values (note ordinate scale changes). About 8 m of the offset seen is due to different reference ellipsoids being used in the two data classes and the rest of the offset is attributable to SEASAT orbit biases, since the SEASAT data displayed here has not been adjusted for orbit bias elimination. The steps (arrows) in the "ship" data in Figure 13(b) are known errors in the geoid-height field and should be disregarded. They are not present in the vertical-deflection field.

Figure 14 gives three samples of SEASAT and "ship" vertical deflections corresponding to the tracks of Figure 13. Here the geoid-height offsets due to the reference ellipsoid and orbit biases do not contribute, but a slope error due either to the SEASAT orbit or the long wavelength model used with the "ship" data would cause an offset of the mean difference from zero. The differences are plotted in Figure 15 (note different ordinate scales), and there appears to be zero offsets of up to about 0.5 arc sec. A further breakdown in the comparison is interesting. Ocean areas can be characterized by the amount and scale of geodetic activity as rough or smooth provinces (Reference 14). Figure 14 (a) and (c) are samples of a smooth province while Figure 14(b) is from a rough province.

If orbit bias adjustments are made to the SEASAT data, the differences in reference ellipsoids taken into account, and the comparisons grouped into smooth and rough geodetic provinces, the following table gives the statistics of the comparisons:

Table 5. RMS Differences Between SEASAT and Ship Data

	Smooth(10 segments)	Rough(5 segments)
Geoid height	1.0 m	1.5 m
Vertical deflection	0.6 arc sec	1.3 arc sec

CONCLUSIONS

This analysis of SEASAT radar altimeter data has shown that SEASAT was capable of superb performance in providing data for ocean geodetic studies and its premature failure was a great loss to ocean geodetic science.

The largest source of error in the determination of geoid heights was orbit error, but this was of very long wavelength and could be minimized by various procedures such as averaging on repeat tracks or local intersection analysis. Orbit error caused negligible error in vertical deflection.

Ice or land falling within the altimeter footprint could cause large errors in both geoid height and vertical deflection. This was known beforehand, and the analysis has shown that the NSWC procedures for eliminating such

contaminated data needs to be improved for follow-on altimeter satellites such as GEOSAT. On occasion, other seemingly random errors have been discovered in the geoid height and/or vertical-deflection results. These are thought to be due to local environmental conditions such as heavy rainstorms, and the present analysis has shown the accuracy of the geodetic data produced under normal open-ocean conditions over a good range of sea states and the values of various parameters (e.g., range noise, AGC σ_{AGC}, SWH, σ_{SWH}, etc.) expected under nominal conditions. The estimates of the accuracy obtainable from a large, well-edited set of SEASAT data are the following:

Geoid height	0.5-1.5 m rms
Vertical deflection	0.5-2.0 arc sec rms

These estimates reflect the inclusion in the data of many local environmental conditions, such as ocean currents and weather systems, whose effects are difficult or impossible to remove at the current level of knowledge. The major contributor to the geoid-height error is the orbit uncertainty.

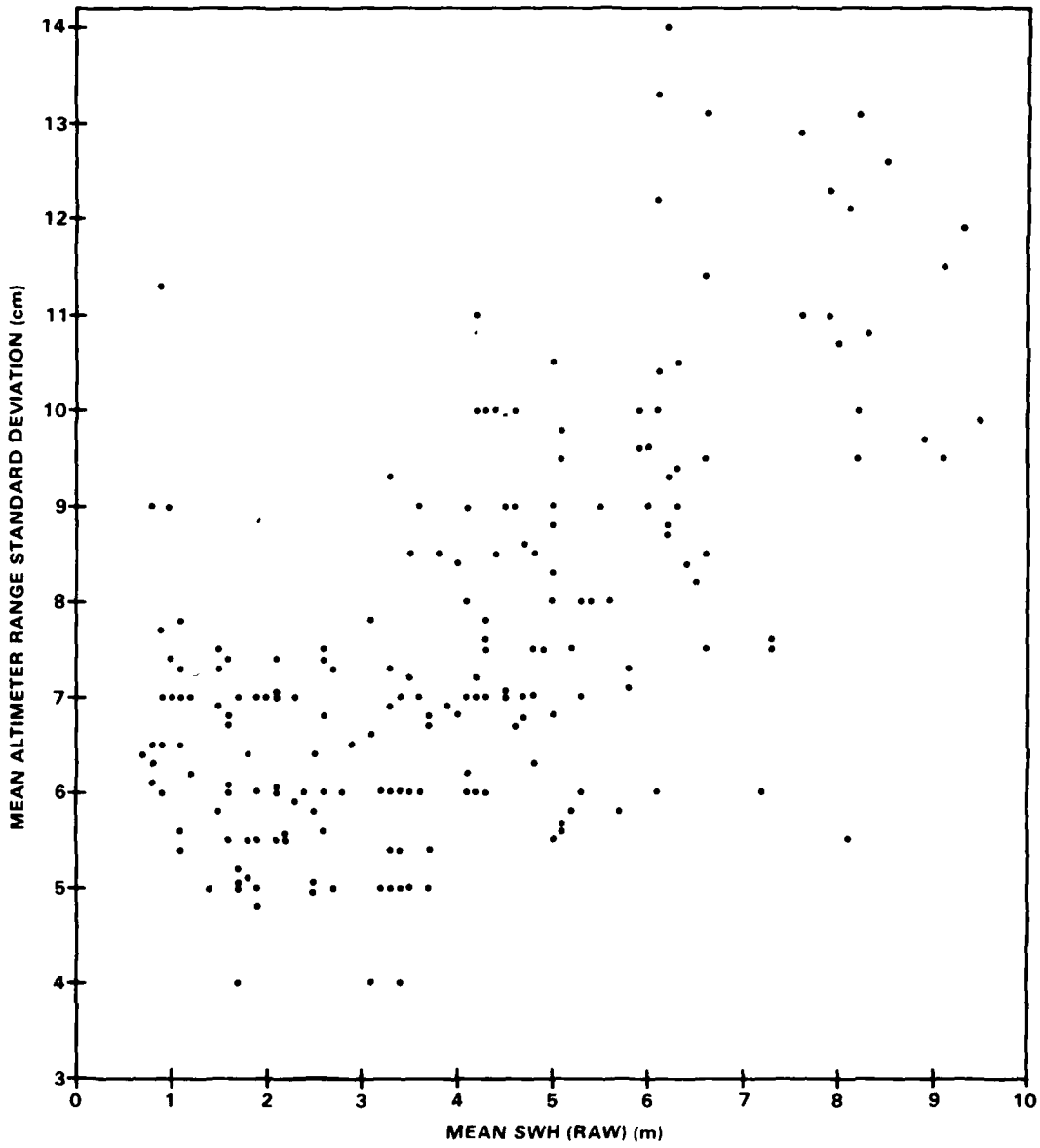

Figure 1. Altimeter Range Noise Versus SWH

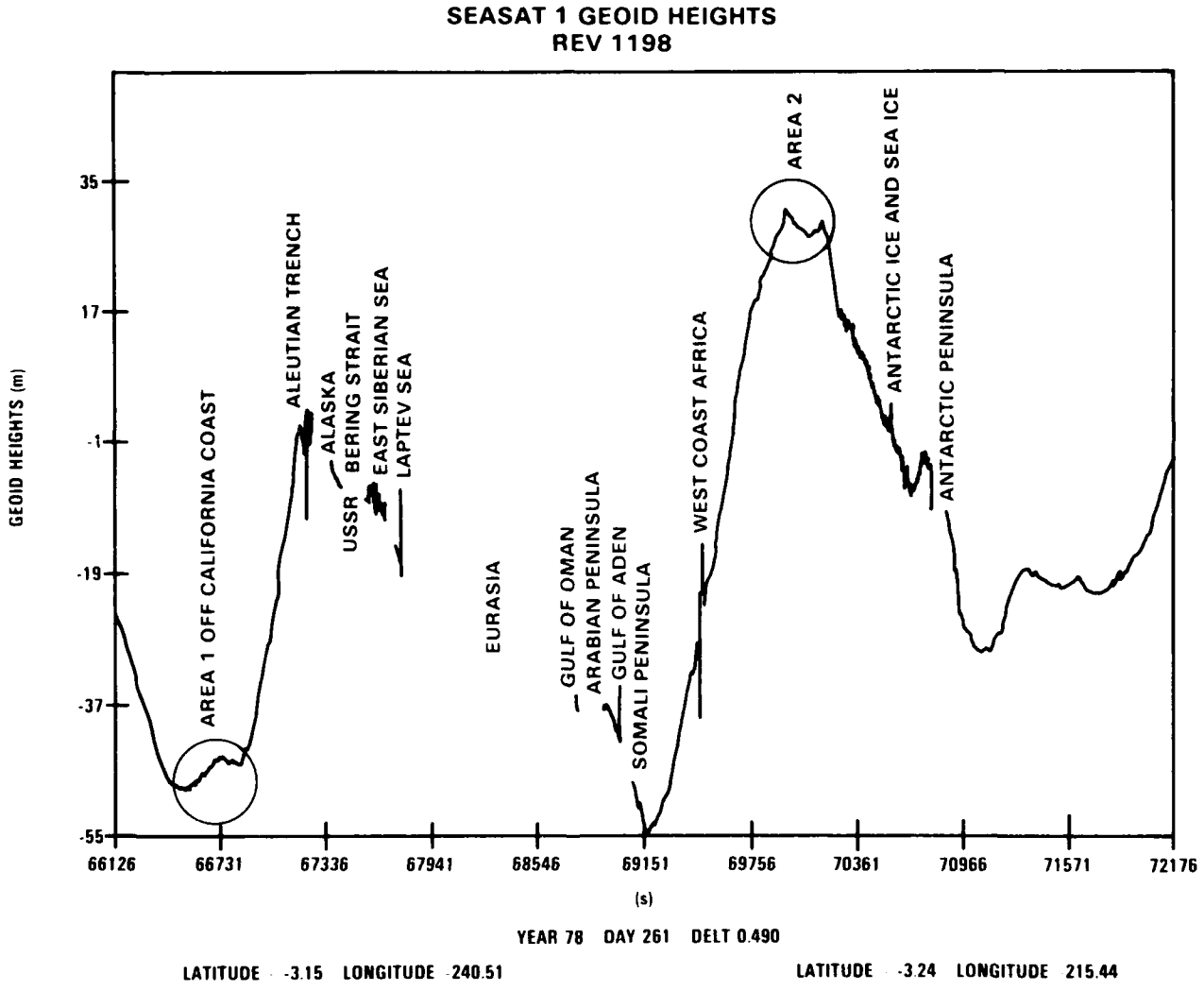

Figure 2. Geoid-Height Plot of the Repeat-Track Sequence (Revolution 1198)

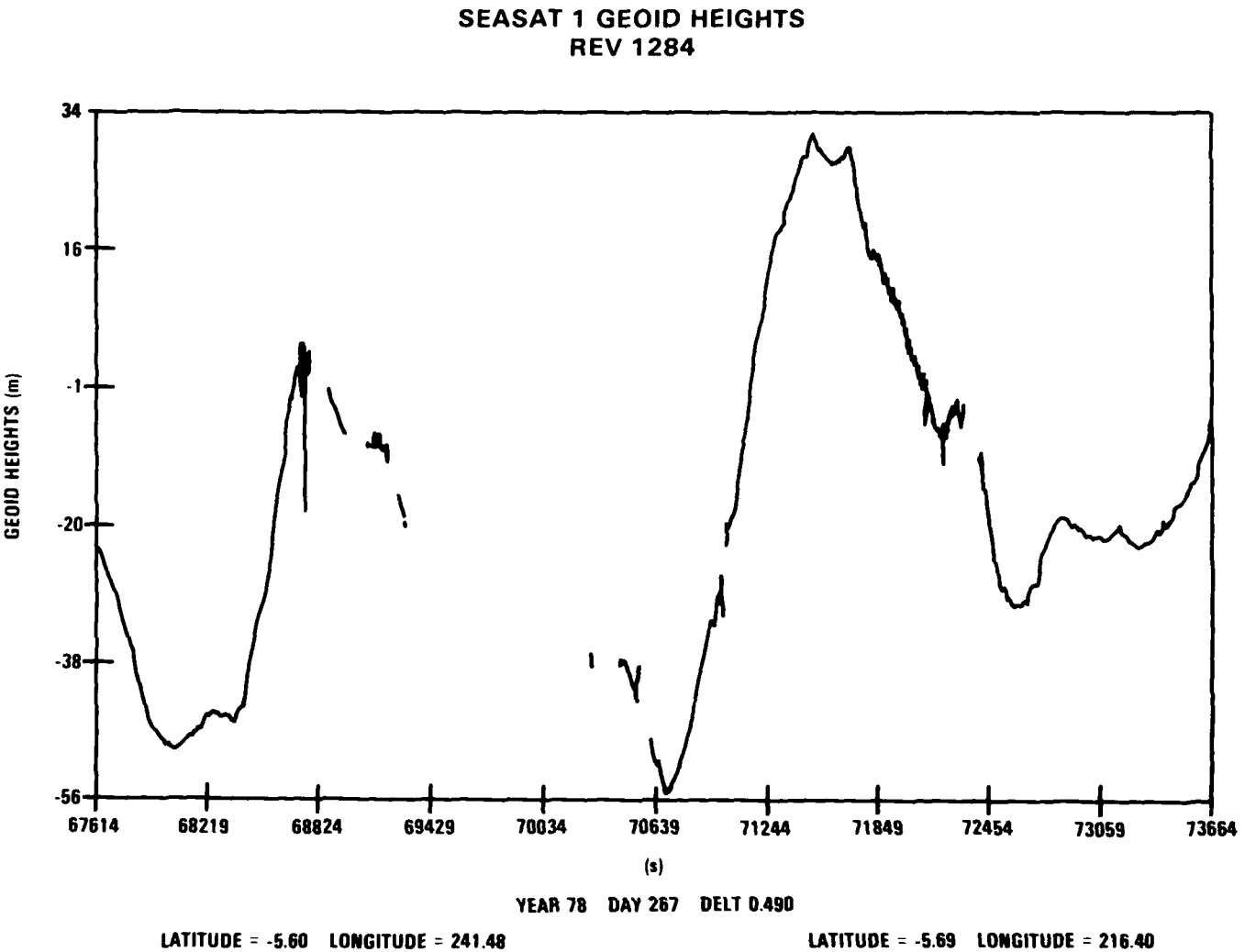

Figure 3. Geoid-Height Plot of the Repeat-Track Sequence (Revolution 1284)

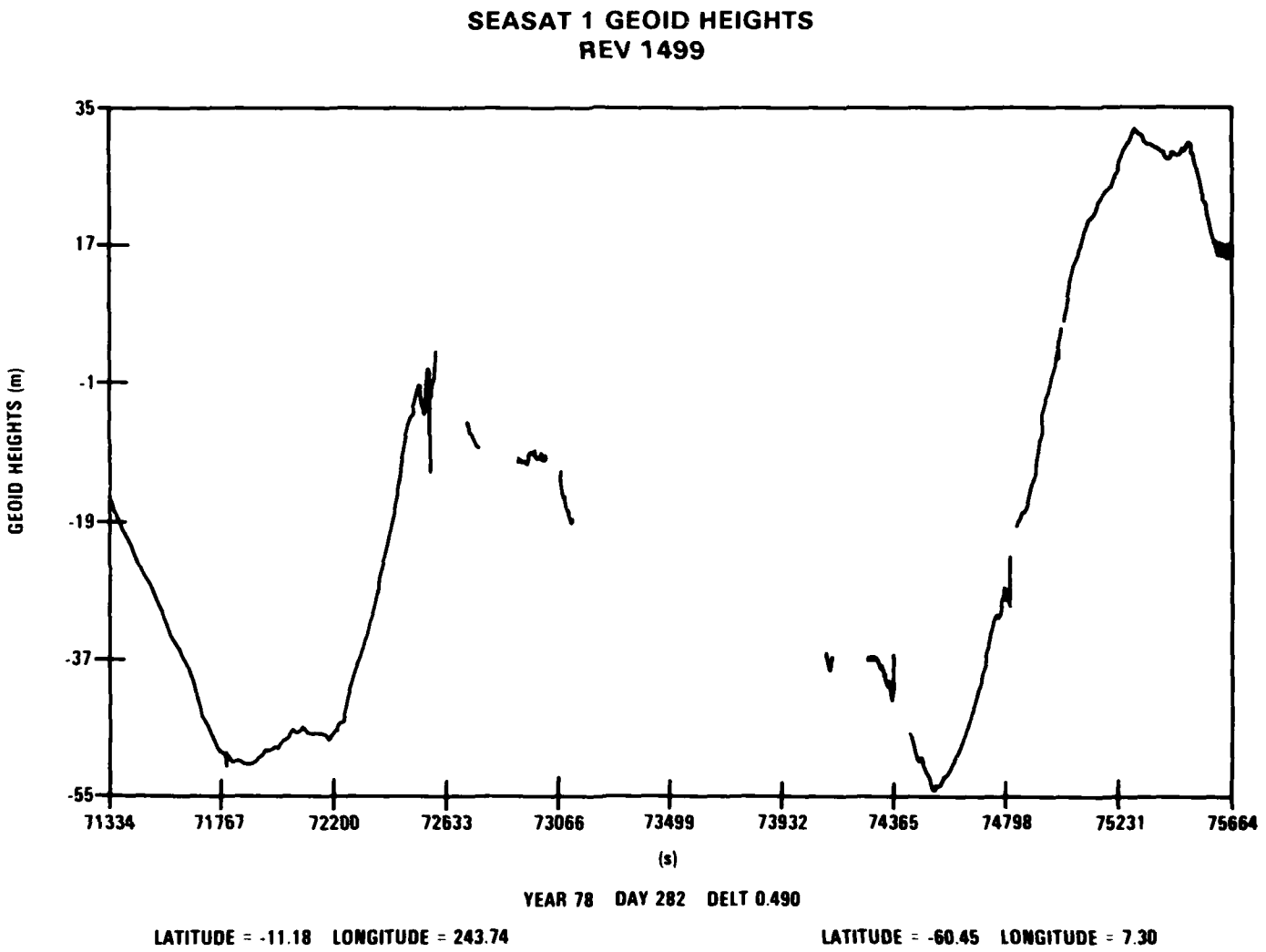

Figure 4. Geoid-Height Plot of the Repeat-Track Sequence (Revolution 1499)

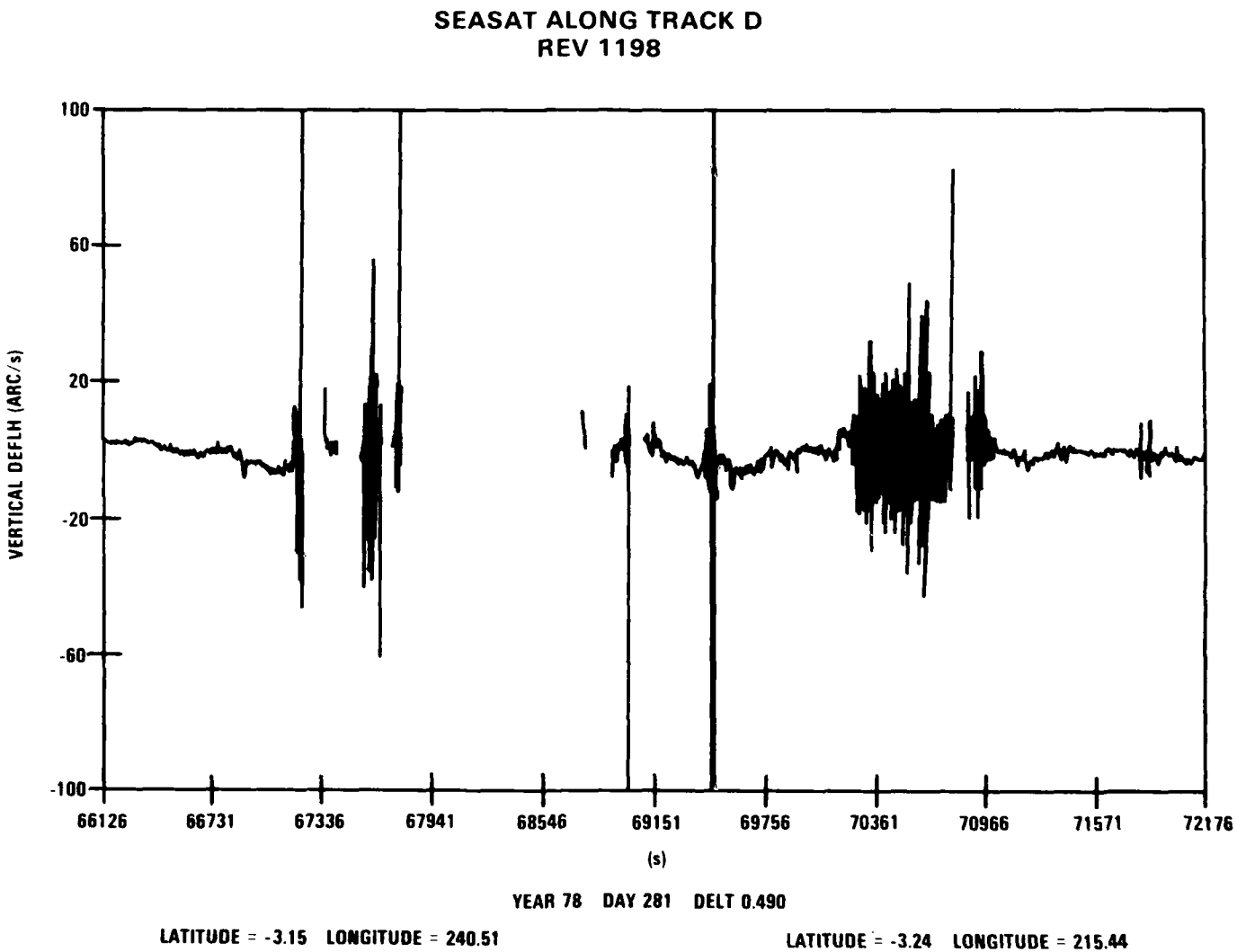

Figure 5. Along-Track Vertical Deflection (Revolution 1198)

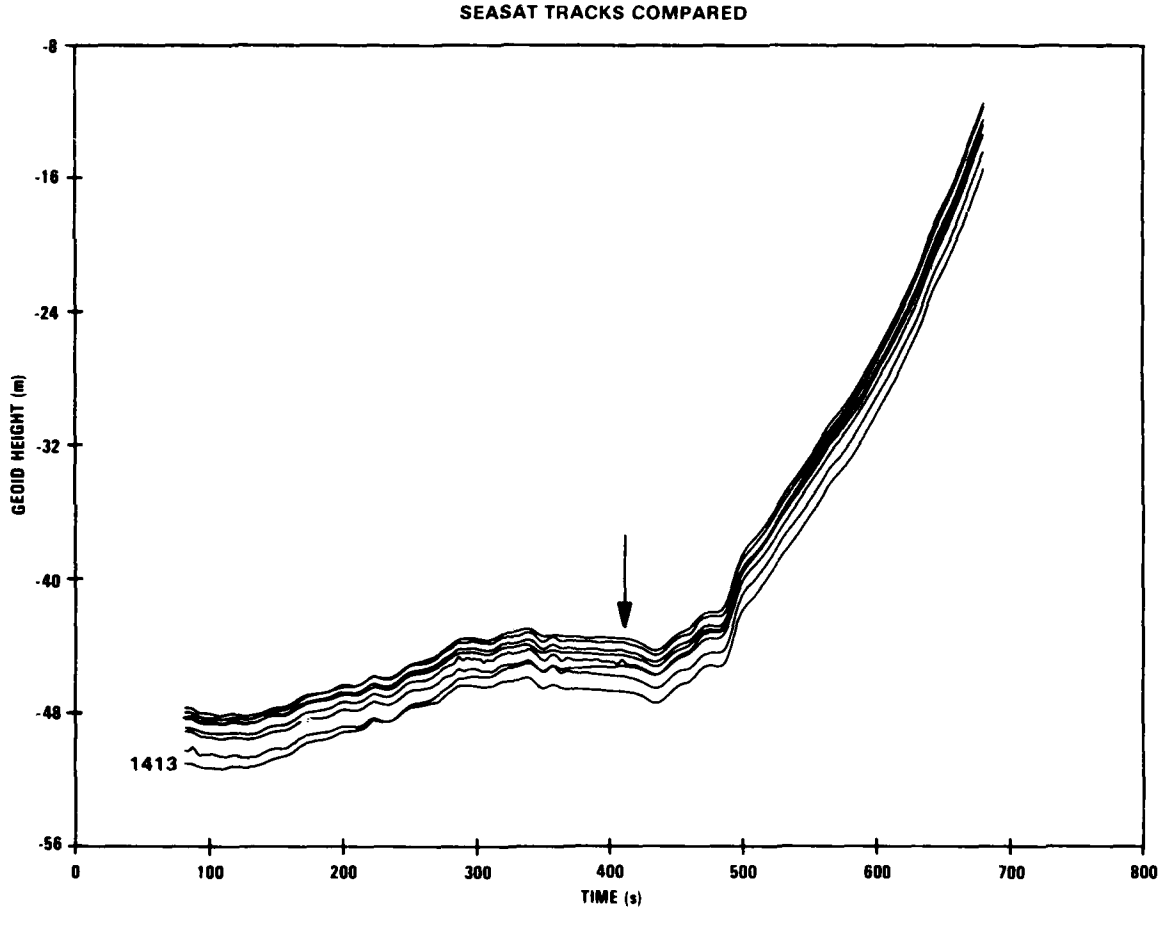

Figure 6. Area 1 Geoid Heights Versus Arbitrary Time Scale

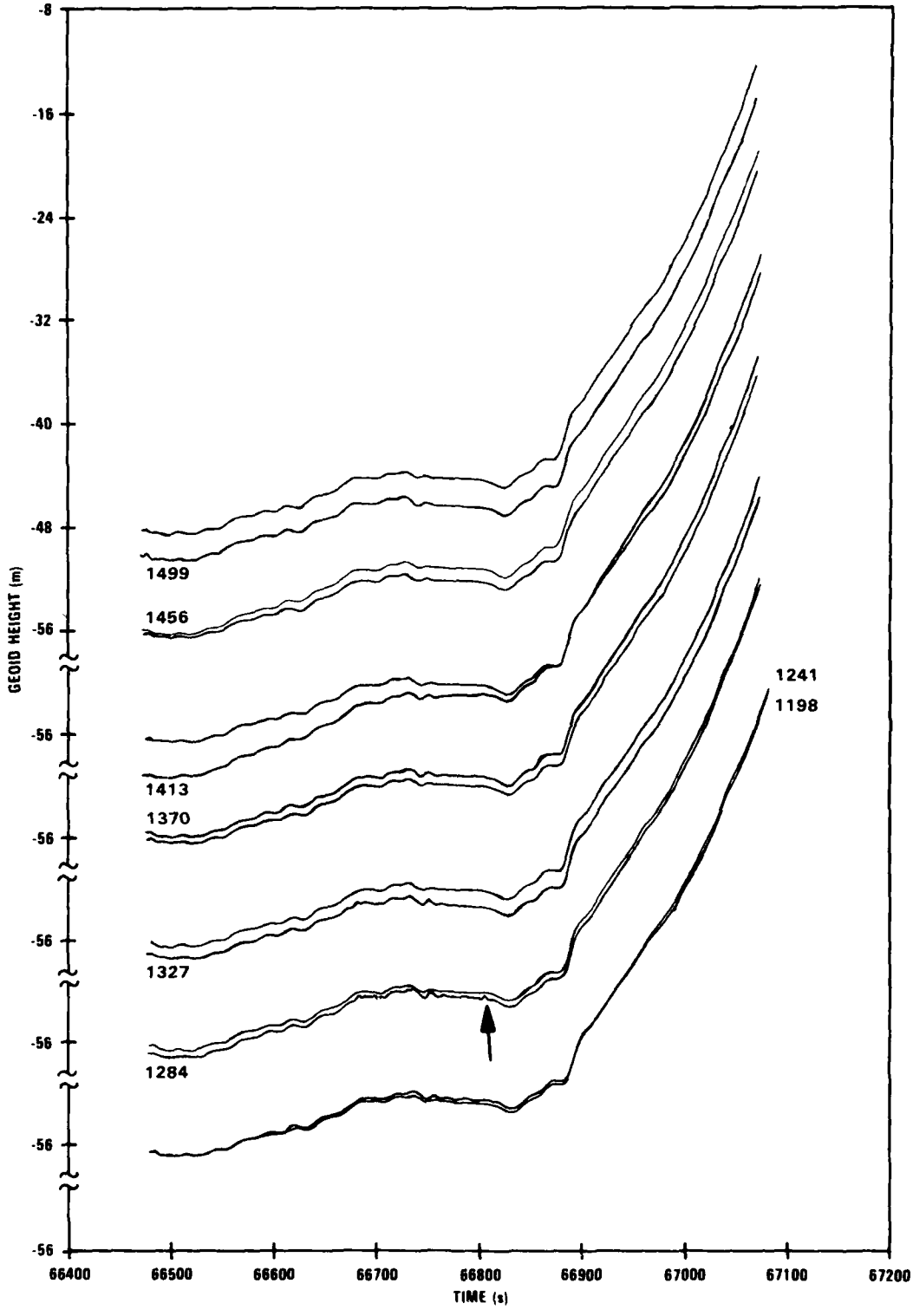

Figure 7. Area 1 Geoid Heights Comparison With Revolution 1198

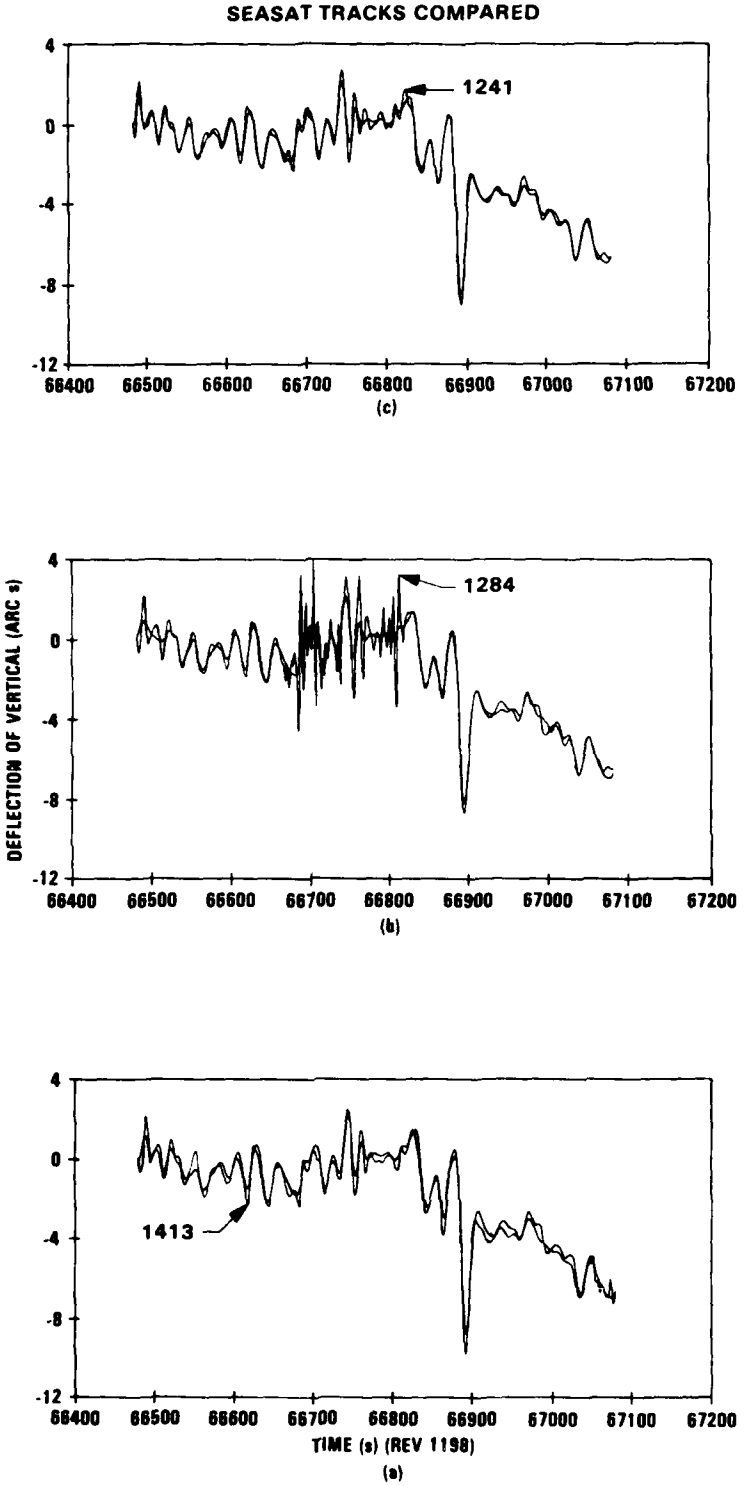

Figure 8. Along-Track Vertical Deflection Plots, Area 1

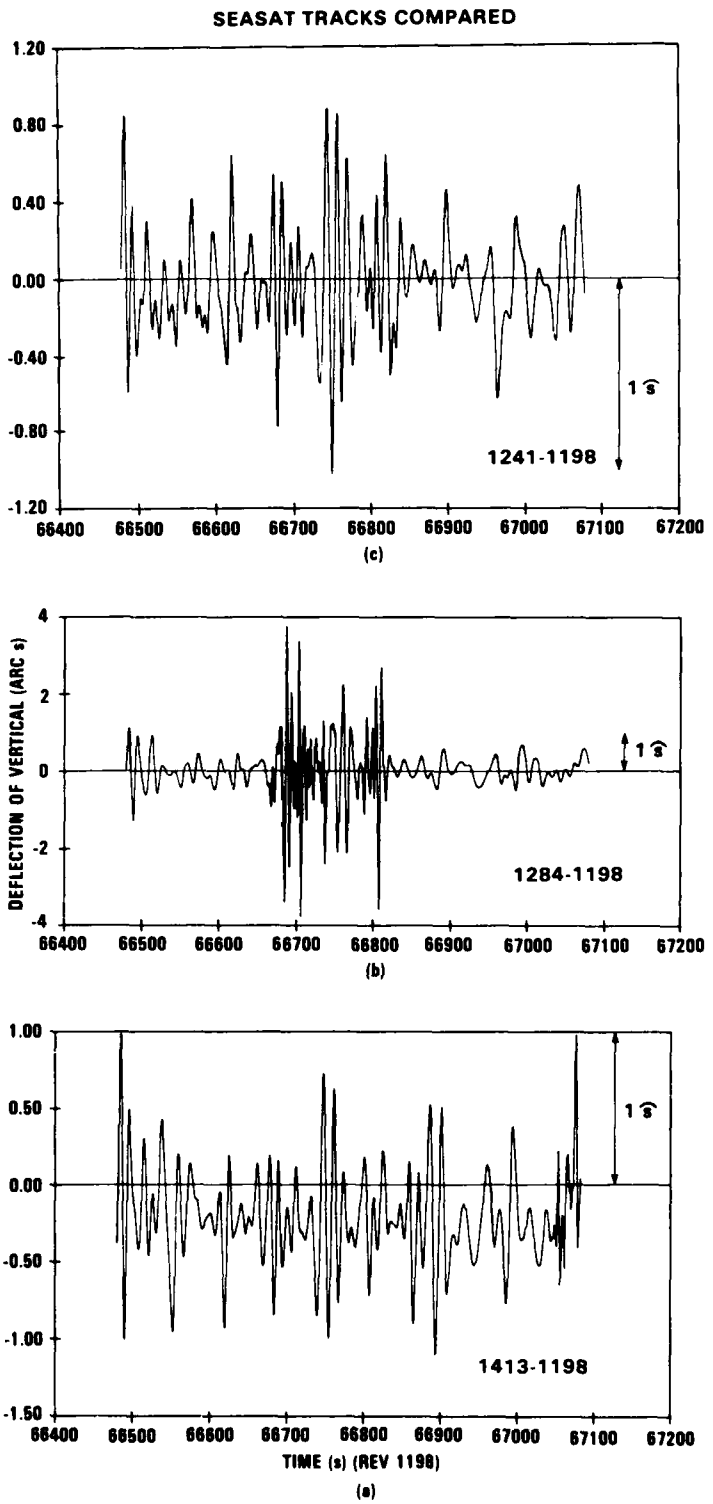

Figure 9. Vertical Deflection Differences, Area 1

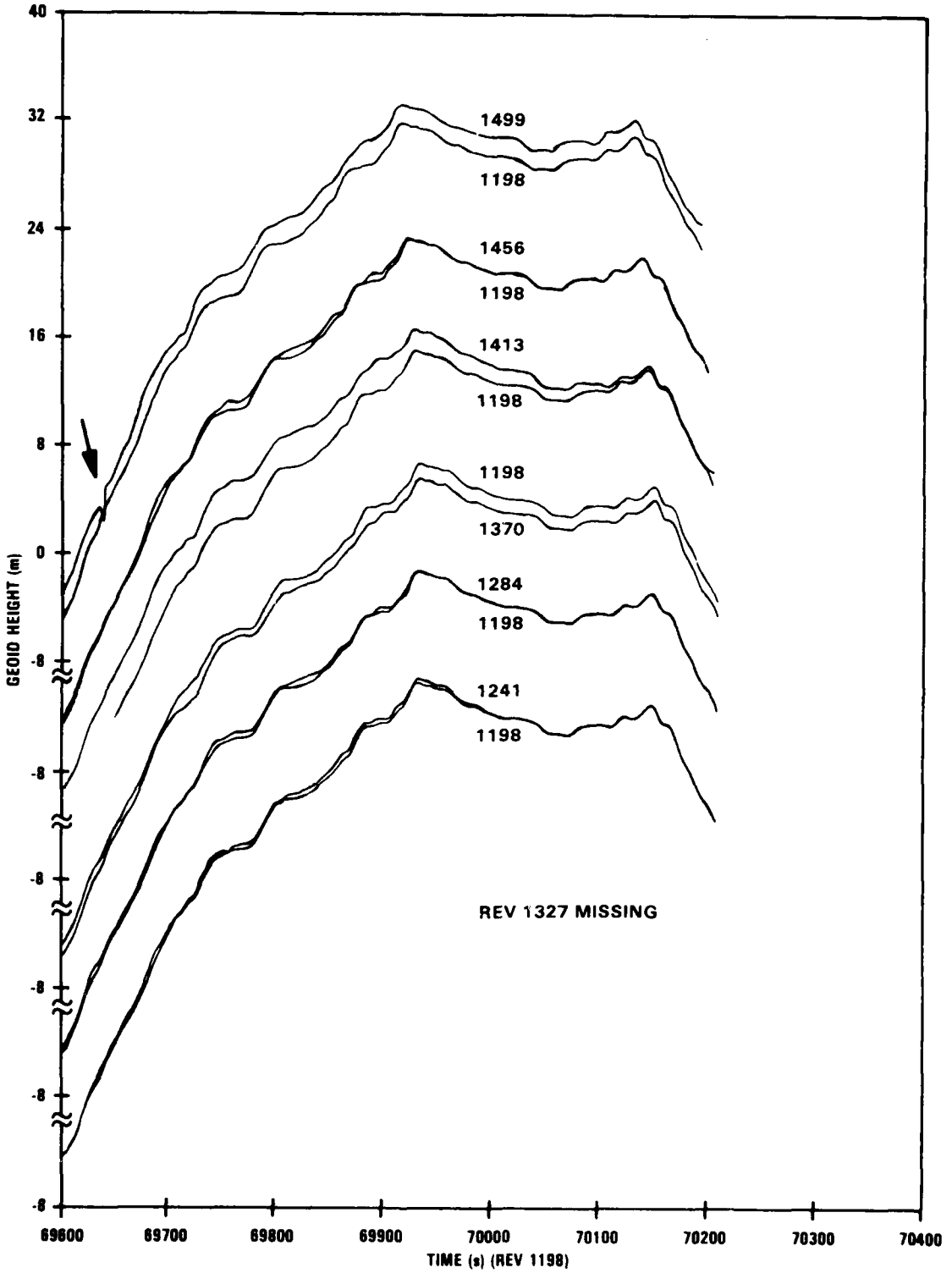

Figure 10. Geoid Heights Comparison, Area 2

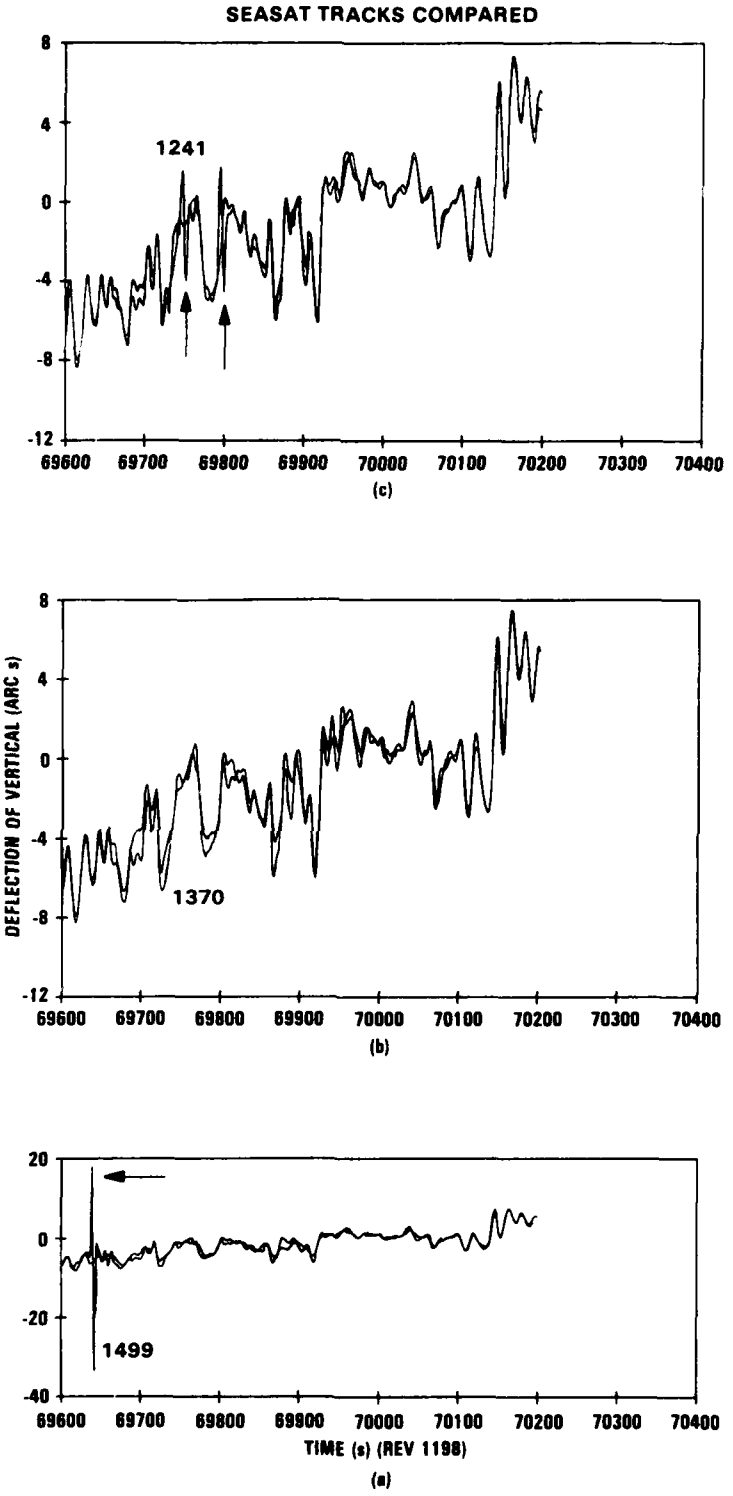

Figure 11. Vertical Deflection, Area 2

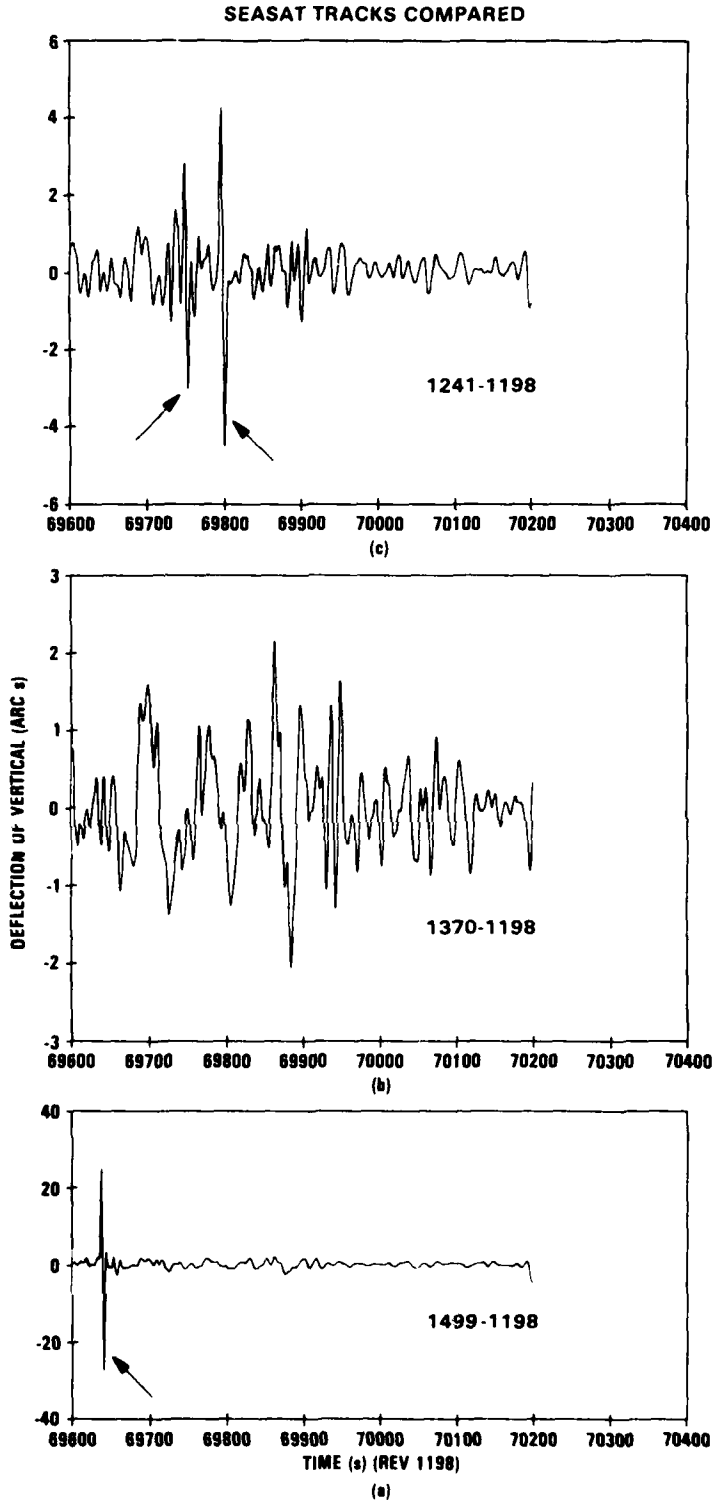

Figure 12. Vertical Deflection Differences, Area 2

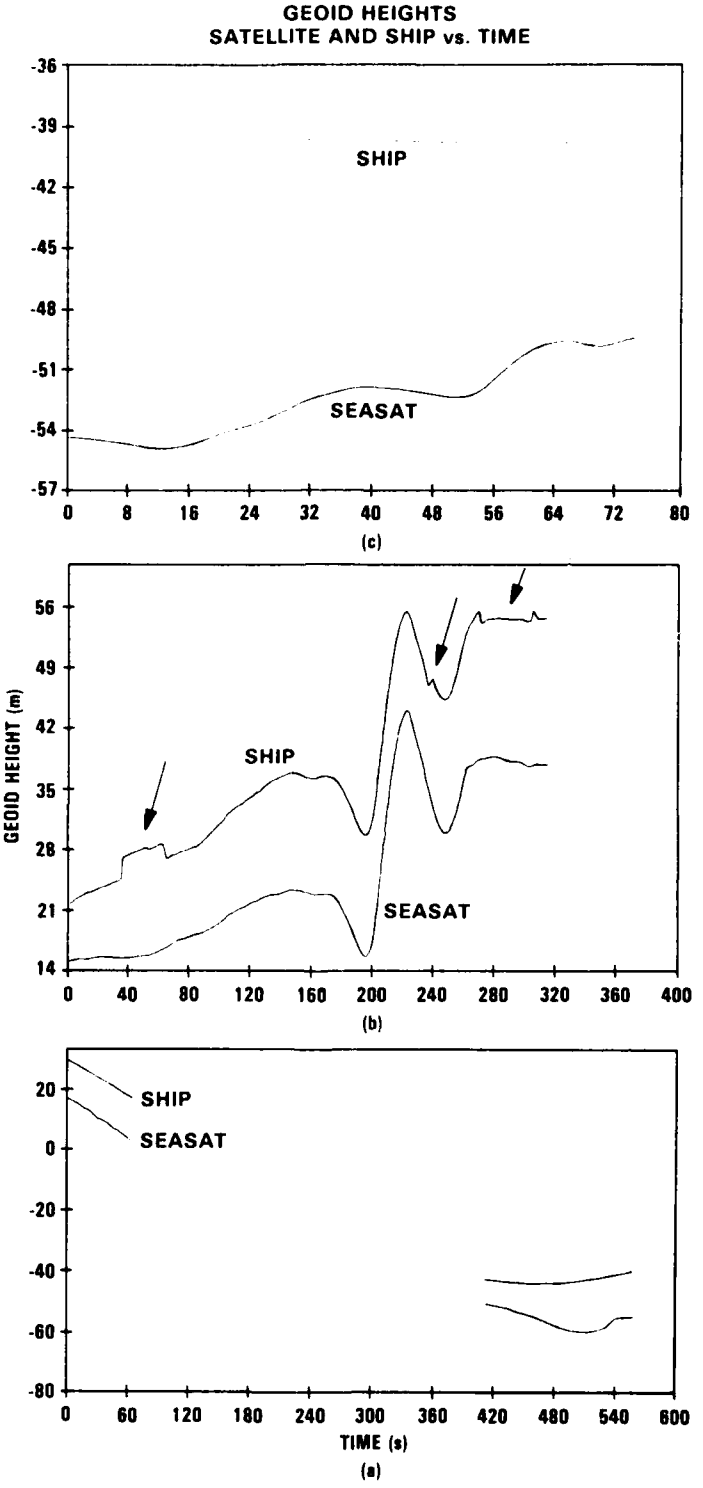

Figure 13. SEASAT and "Ship" Geoid Height Values

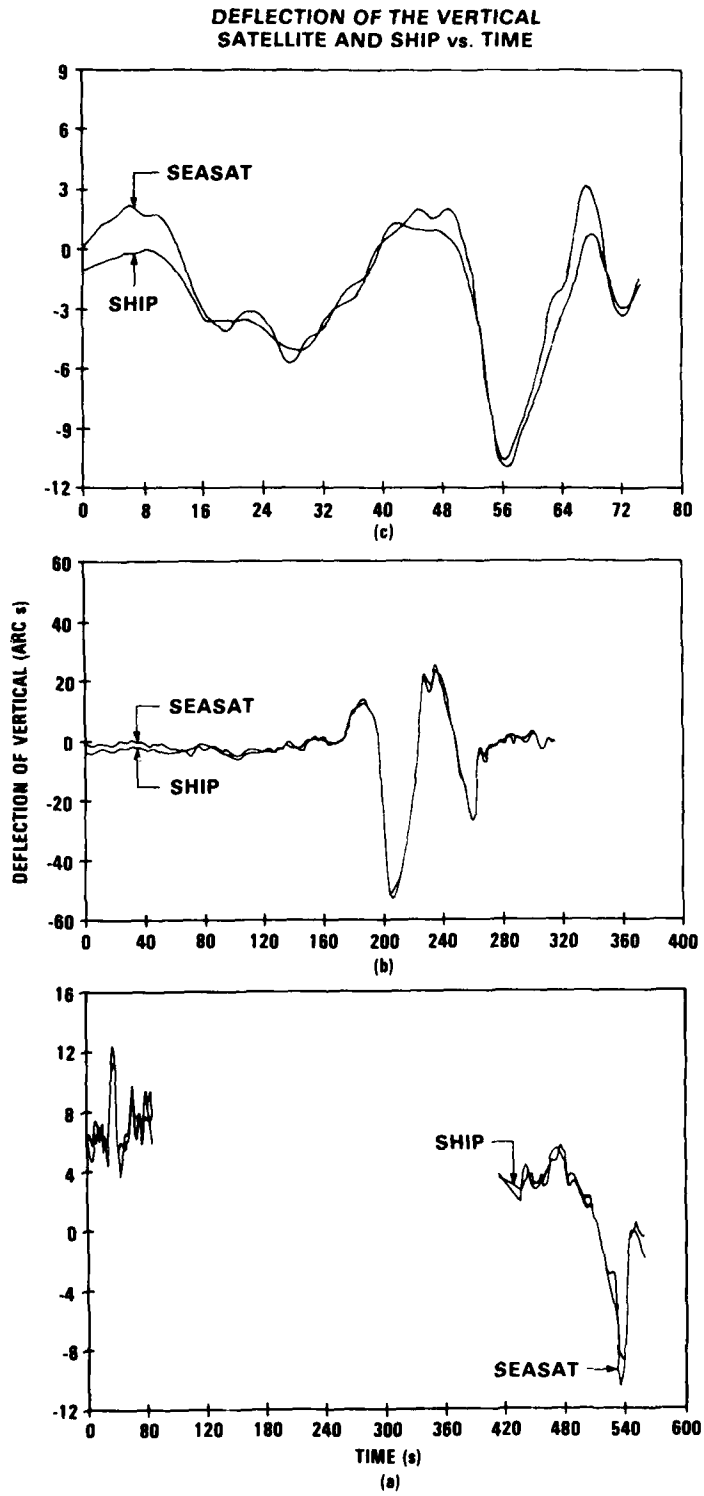

Figure 14. SEASAT and "Ship" Vertical Deflections

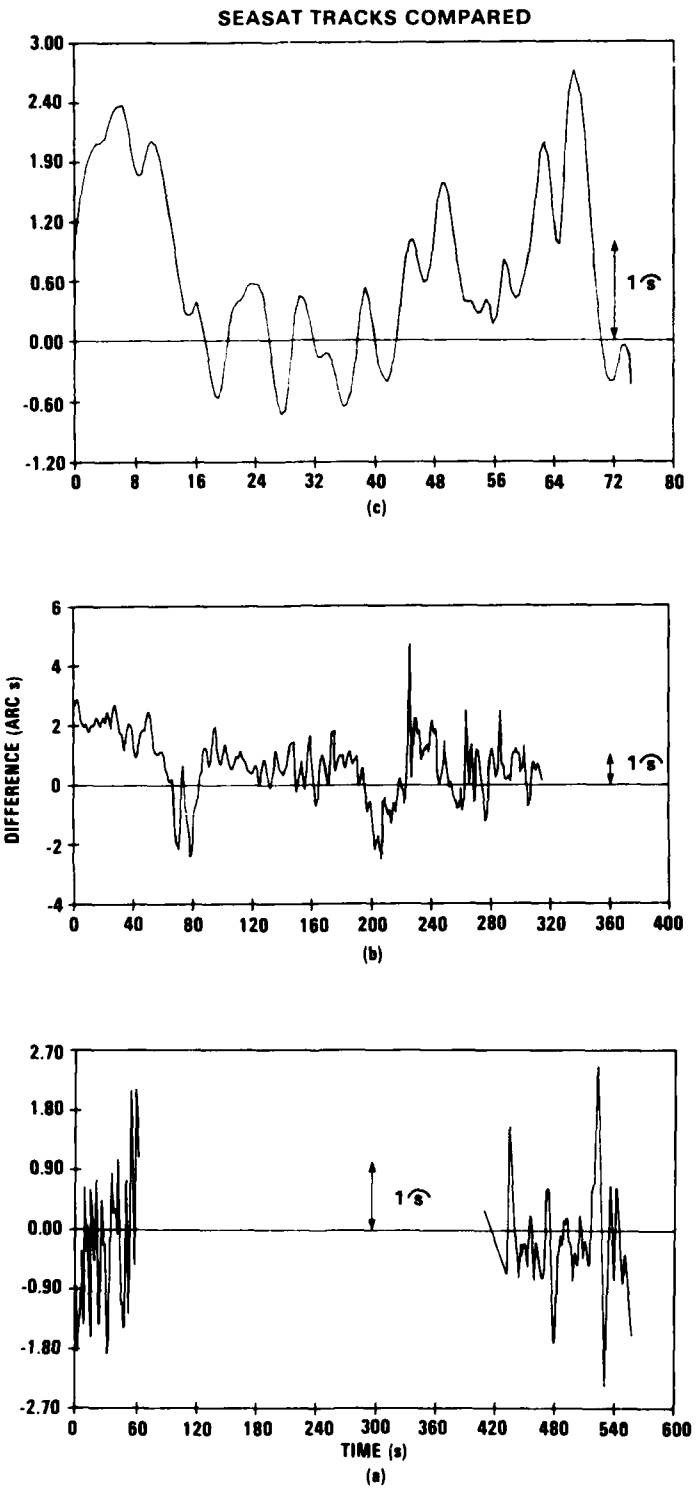

Figure 15. SEASAT and "Ship" Vertical Deflection Differences

REFERENCES

1. Special Issue on the SEASAT-1 Sensors, *IEEE Journal of Oceanic Engineering*, Vol OE-5, No. 2, April 1980.

2. E. W. Schwiderski, Global Ocean Tides, Part II: *The Semidiurnal Principal Lunar Tide (M_2), Atlas of Tidal Charts and Maps*, NSWC TR 79-414 (Dahlgren, Va., December 1979). Also parts III through X.

3. Joseph M. Futcher, Jr., *Program Maintenance Manual for SEASAT Reduce Program*, NSWC TN 80-96 (Dahlgren, Va., April 1980).

4. Gladys B. West, *SEASAT Satelite Radar Altimetry Data Processing System*, NSWC TN 81-26 (Dahlgren, Va.)

5. Elodie S. Colquitt, Carol W. Malyevac and Richard J. Anderle, Doppler Computed SEASAT Orbits, *The Journal of the Astronautical Sciences*, Vol. XXVIII, No. 4, October-December 1980.

6. J. Lorell, *Algorithm Development Facility Altimeter Sensor Algorithm Specifications*, JPL 622-202, June 1979.

7. *Accuracy Assessment of the SEASAT Orbit and Height Measurement*, edited by B. D. Tapley et al, Institute for Advanced Study in Orbital Mechanics, University of Texas at Austin, IASOM TR 79-5, October 1979.

8. L. Ralph Gibson, *Some Expansions for an Electromagnetic Wave Propagating through a Spherically Symmetric Refracting Medium*, NSWC/DL TR-3344 (Dahlgren, Va., June 1975).

9. Jack Lorell, Elodie Colquitt and Richard J. Anderle, *Altimeter Height Correction for Ionosphere*, In press.

10. J. P. Hollinger, *SEASAT Altimeter Atmospheric Range Correction*, NRL Memorandum Report 4342, September 1980.

11. G. B. West, T. I. Hicks and R. B. Manrique, *NSWC/DL Filtering of GEOS-3 Radar Altimeter Data*, NSWC/DL TR-3686 (Dahlgren, Va., November 1977).

12. S. L. Smith III, T. I. Hicks, G. B. West and P. Ugincius, "Analysis of SEASAT Radar Altimeter Observations," Presentation at 1979 Spring Meeting of American Geophysical Union, May 1979.

13. *SEASAT Gulf of Alaska Workshop Report*, Volume 1, Panel Reports, JPL 622-101, April 1979.

14. Thomas M. Davis, *Theory and Practice of Geophysical Survey Design*, NAVOCEANO Report RP-13, October 1974.

DISTRIBUTION

Defense Technical Information Center
Cameron Station
Alexandria, VA 22314 (12)

Library of Congress
Attn: Gift and Exchange Division
Washington, DC 20540 (4)

Director Defense Mapping Agency
U. S. Naval Observatory
Bldg 56
Attn: O. W. Williams
C. Martin
P. M. Schwimmer
W. Senus
R. Berkowitz
Washington, DC 20360

Defense Mapping Agency
Aerospace Center
Attn: R. Ballew (5)
L. B. Decker
M. Schultz
K. Nelson
St. Louis, MO 63118

Defense Mapping Agency
Hydrographic/Topographic Center
Attn: H. Heuerman
Washington, DC 20315

Commander
Naval Oceanographic Office
NSTL Station
Attn: T. Davis (5)
J. Hankins
S. Odenhal
Bay St. Louis, MS 39522

Oceanographer of the Navy
U. S. Naval Observatory
Bldg 1
Washington, DC 30360 (2)

Naval Oceanography Division
U. S. Naval Observatory
Bldg 1
Attn: H. Nicholson - Code NOP-952
Washington, DC 20360

NASA - Goddard Space Flight Center
Attn: J. W. Siry
F. O. Vonbun
D. E. Smith
J. G. Marsh
R. Kolenkiewicz
Greenbelt, MD 20771

Jet Propulsion Laboratory
4800 Oak Grove Drive
Attn: W. E. Giberson
P. Rygh
A. Loomis
J. Lorell (2)
G. Born (2)
Pasadena, CA 91103

NOAA - National Ocean Survey/National Geodetic Survey
6001 Executive Blvd.
Attn: B. H. Chovitz
B. Douglas
C. Goad
J. Diamante
Rockville, MD 20852

NOAA - Pacific Marine Environmental Laboratory
Attn: J. Apel
M. Byrne
Seattle, WA 98105

NOAA - National Environmental Satellite Service
5100 Auth Road
Attn: J. W. Sherman III
P. S. DeLeonibus
P. McClain
Camp Springs, MD 20031

NOAA - Environmental Research Laboratories
Attn: L. S. Fedor
C. Rufenach
Boulder, CO 80302

Applied Physics Laboratory
Johns Hopkins University
Attn: John McArthur (2)
C. Kilgus (2)
Laurel, MD 20810

Deputy Chief of Naval Operations
Attn: NOP-21D (Tomajczyk)
Washington, DC 20350 (2)

Strategic Systems Project Office
Attn: SP20123 (P. Fisher)
Washington, DC 20376 (5)

Office of Naval Research
800 N. Quincy St.
Attn: P. C. Badgley
Arlington, VA 22217 (2)

Director Naval Research Laboratory
Attn: V. Noble
B. Yaplee
L. Choy
D. Hammond
A. Uliana
D. Chen
J. Hollinger
P. Vogt
Washington, DC 20375

Commander
Fleet Numerical Oceanography Center
Attn: E. Schwartz
J. Cornelius
O. Lovel
L. Clark
Monterey, CA 93940

Air Force Geophysical Laboratory
L. G. Hanscom Field
Attn: G. Hadgigeorge
Bedford, MA 01730

NASA Headquarters
600 Independence Avenue, S.W.
Attn: W. F. Townsend (3)
L. Greenwood
C. Finley
Washington, DC 20546

NASA - Wallops Flight Center
Attn: J. McGoogan
R. Stanley
C. Purdy
Wallops Island, VA 23337

University of Texas
Dept. of Aerospace Engineering
Attn: B. D. Tapley (5)
B. Schutz
Austin, TX 78712

Scripps Institution of Oceanography
Attn: R. Steward
R. L. Bernstein
LaJolla, CA 92093

Woods Hole Oceanographic Institute
Attn: J. A. Whitehead
Woods Hole, MA 02543

Institute of Marine and Atmospheric Science
City University of New York
Attn: W. J. Pierson
New York, NY 10031

Department of Geodetic Science
Ohio State University
Attn: R. Rapp
Columbus, OH 43210

Local: E41
K05
K10 (50)
K12 (20)
K40 (5)
K50 (5)
X210 (6)

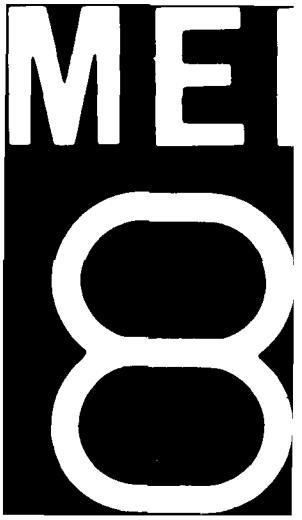
MEI
8